Cement and Concrete Research 79 (2016) 45–48

Contents lists available at ScienceDirect

Cement and Concrete Research

journal homepage: http://ees.elsevier.com/CEMCON/default.asp

Short communication

Nanoscale heterogeneities in a fractured alkali-activated slag binder: A helium ion microscopy analysis

Antoine E. Morandeau [a,b], Jeffrey P. Fitts [a], Hang D. Lee [c,d], Samir M. Shubeita [c,d], Leonard C. Feldman [c,d], Torgny Gustafsson [c,d], Claire E. White [a,b,*]

[a] Department of Civil and Environmental Engineering, Princeton University, Princeton, NJ, USA
[b] Andlinger Center for Energy and the Environment, Princeton University, Princeton, NJ, USA
[c] Department of Physics and Astronomy, Rutgers University, Piscataway, NJ, USA
[d] Institute for Advanced Materials, Devices, and Nanotechnology, Rutgers University, Piscataway, NJ, USA

ARTICLE INFO

Article history:
Received 28 November 2014
Accepted 27 July 2015
Available online 13 August 2015

Keywords:
Helium ion microscopy
Alkali activated cement
Microstructure
Granulated blast-furnace slag
Drying

ABSTRACT

Helium ion microscopy is used to provide new insight into the nano- and microscale morphology of cleaved surfaces of alkali-activated slag (AAS), revealing that AAS contains several types of gel with varying surface morphologies after being subjected to D-drying. It is seen that the bulk C-(N)-A-S-H gel is globular in nature in a silicate-activated slag paste while the gel covering the slag particles is foil-like.

1. Introduction

The development of alkali-activated materials (AAMs) is being readily pursued in order to reduce greenhouse gas emissions associated with the manufacture of cementitious materials [1]. AAM binder systems replace ordinary Portland cement (OPC) with industry-derived by-products such as ground-granulated blast furnace slag (GGBS) and coal-derived fly ash. Alkali-activation of these precursors leads to a mechanically hard binder, however, their implementation in the construction industry is hampered by the lack of durability data proving adequate long-term performance. The durability of cement binders is intimately linked with the ability of the binder to resist chemical and mechanical degradation [2]. One example of mechanical degradation is microcracking, where the buildup of internal (compressive) forces due to drying combined with a non-uniform drying front can result in tensile-induced surface cracking of the cement binder [3].

Recent work on AAMs has shown that GGBS-based pastes are more prone to microcracking compared to metakaolin and fly ash-based pastes [4,5]. This reveals that the chemistry of the gel binder, particularly the presence of calcium in the GGBS-based gel phases, may play an important role in governing the extent of microcracking. In particular, there are differences in the nature of the percolated pore network associated with sodium-alumino-silicate-hydrate (N-A-S-H) gel in metakaolin and fly ash-activated pastes and calcium-alumino-silicate-hydrate (C-A-S-H) gel in GGBS-activated pastes, where the size of the percolating pores diminishes as the system moves toward a calcium-rich environment [6]. Hence, using GGBS in AAMs (together with a sodium silicate-based activator) leads to the formation of gel pores (less than 10 nm in diameter) within the C-A-S-H gel matrix together with a depercolated capillary pore network [7]. On the other hand, in N-A-S-H gel systems (metakaolin and fly ash) there is a lack of gel pores due to the absence of calcium, and therefore it is the capillary network that is percolated and controls permeability (pores larger than 10 nm) [8]. This raises the question as to whether this relatively high content of bound water in the calcium-based hydrate gel compared to an aluminosilicate gel is responsible in part for microcracking in GGBS-based pastes, specifically via the removal of the bound water and the reduction in gel volume (shrinkage). Drying-induced shrinkage does not necessarily lead to microcracking, since if the body dries uniformly then there are only compressive stresses acting on the body. However, if there is a drying front present, where the center of the sample is fully-saturated while the outer regions are dry, this restrained shrinkage can lead to a significant buildup in tensile stresses acting at the surface. If these stresses exceed the tensile strength of the paste, then cracking occurs [3].

A previous investigation has revealed that the activator chemistry also plays an important role in controlling the percolated pore network

* Corresponding author at: Department of Civil & Environmental Engineering, Princeton University, Princeton, NJ 08544, USA. Tel.: +1 609 258 6263; fax: +1 609 258 2799.
E-mail address: whitece@princeton.edu (C.E. White).

http://dx.doi.org/10.1016/j.cemconres.2015.07.007
0008-8846/

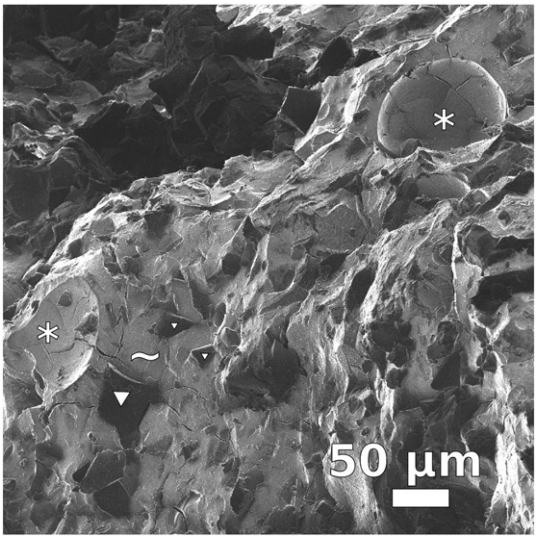

Fig. 1. HIM image of the fractured sample of alkali-activated GGBS: air bubble led to the formation of concave spherical voids (*). The black angular-shaped particles (∇) are unreacted GGBS coated in C-(N)-A-S-H gel (charging under the helium beam) embedded in a continuous gel matrix of light gray C-(N)-A-S-H gel (~).

size in AAMs, with silicate-activated binders leading to lower permeability values measured using a pressure differential (beam-bending technique [9,10]) [7]. These results correlated with the reduction in pore size measured using mercury intrusion porosimetry when free silica is available in the activating solution. Hence, although it is known that this free silica is advantageous for early strength development in AAMs [11], there are deleterious effects due to the small pore size of the percolated pore network and therefore significant pore pressures associated with drying. However, it is unknown if the gel porosity is uniform throughout the paste matrix at the nanoscale, or if certain regions of the paste are more susceptible to drying compared to others.

One experimental technique capable of investigating the changes in microstructure that occur during microcracking in cements is scanning electron microscopy (SEM). Investigations have been carried out using SEM to study the microstructure of alkali-activated GGBS (AAS) [12,13]. San Nicolas et al. [12] recently used SEM coupled with energy-dispersive X-ray spectroscopy (EDX) on polished samples to investigate the microstructure of 7-year old sodium silicate-activated GGBS. The images revealed the presence of Liesegang rings around the partially-dissolved GGBS particles, which indicate that the growth of the complex 'inner' product gel surrounding the GGBS particles occurs in supersaturation-depletion Ostwald-type cycles, while the 'outer' product is seen as a porous alkali-activated paste. Although the reaction product hydrotalcite ($Mg_6Al_2CO_3(OH)_{16}\cdot 4H_2O$) was not observed in the sample [12], TEM morphology suggests that the existence of magnesium/aluminum-rich phases may be intermixed with aluminum-substituted calcium-silicate-hydrate (C-A-S-H) gel at a much finer length scale (i.e., nanometers as opposed to microns) [14–16]. The microstructure of AAS has been extensively studied in the literature using SEM and TEM, however, nanoscale heterogeneities have not been studied in depth, including the different microstructural morphologies present in AAS for as-cleaved surfaces. This information can be obtained using helium ion microscopy (HIM) [17], which has recently emerged as an ideal technique for accessing the finer morphological surface details for as-cleaved cement surfaces.

In this study HIM is used to investigate the fractured surface morphology of dried AAS. HIM is similar to SEM imaging by detecting secondary electrons but helium ions are used instead of electrons to excite secondary electrons from the sample's surface under investigation. In comparison with SEM, images obtained by HIM result in significantly improved spatial resolution due to the nature of the beam–sample interaction [18]. Energetic helium ions have straight-line trajectories, as they penetrate the solid with less lateral scattering and hence a reduced ionization volume at the surface. This leads to a significant improvement in resolution for HIM imaging [19], and makes this technique ideal for studying as-cleaved surfaces, without the need for additional sample preparation (i.e., polishing) as soon as the sample is able to sustain high vacuum (10^{-7} Torr). However, as with any technique that requires high vacuum, any free water (absorbed or in pores) must be removed so that the vacuum levels can be reached within a reasonable time period. Hence, as is the case for drying-induced microcracking in industrial settings, any paste sample studied using HIM must experience some sort of drying technique that will inevitably remove water from the pores and therefore be prone to cracking [20]. A major advantage of HIM imaging is the easy mitigation of positive surface charging by the use of an electron flood gun, which allows direct imaging of non-conductive samples without the use of a conductive coating required in SEM for polished surfaces.

2. Materials and methods

In this investigation, the AAS sample was synthesized using a sodium silicate solution consisting of anhydrous sodium metasilicate (Na_2SiO_3) powder (Sigma-Aldrich) dissolved in 99.9% D_2O (Sigma-Aldrich). The GGBS precursor was previously characterized in ref. [21]. D_2O was utilized in this investigation due to complementary neutron scattering experiments (unpublished data). The Na_2O dose was 7.0 wt.% (i.e., 7 g Na_2O per 100 g solid GGBS precursor), and a D_2O/GGBS wt. ratio of 0.389 was used. After 14 days of curing in a sealed

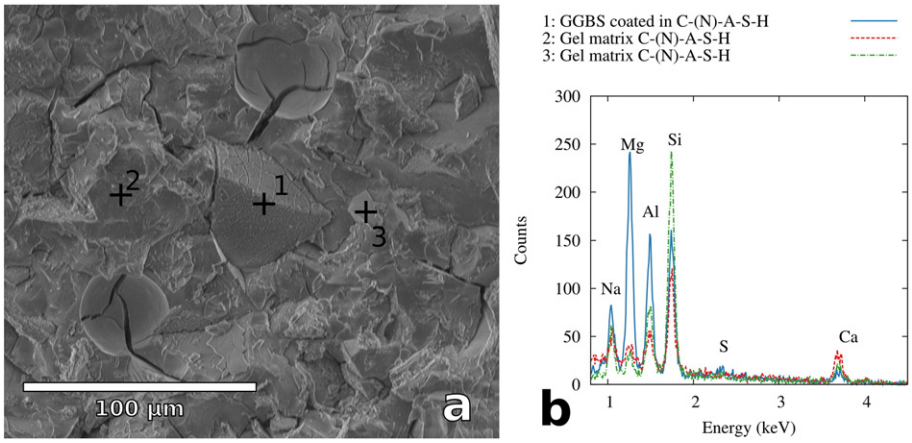

Fig. 2. SEM (a) and EDX (b) analysis of an angular particle identified as GGBS coated in C-(N)-A-S-H (1) and the surrounding C-(N)-A-S-H gel (2 and 3).